Available online at www.sciencedirect.com
ScienceDirect
Trans. Nonferrous Met. Soc. China 33(2023) 2853−2865
Transactions of Nonferrous Metals Society of China
www.tnmsc.cn

Migration regularity and control of silver inclusions during copper electrorefining process

Wen-yu FENG, Hua-zhen CAO, Yu-kun SHEN, Sheng-hang XU, Hui-bin ZHANG, Guo-qu ZHENG

College of Materials Science and Engineering, Zhejiang University of Technology, Hangzhou 310014, China

Received 16 February 2022; accepted 10 May 2022

Abstract: The reduction behavior of free Ag^+ was analyzed by thermodynamic calculation, and the control technique of Ag inclusions was studied by electrolysis experiments. The results show that the discharge reduction of free Ag^+ is inevitable. The entrainment of floating anode slime formed by As, Sb and Bi is the key factor for the inclusions of AgCl and Ag colloidal particles in cathode copper. Sb_2O_3 is adopted to purify the copper electrolyte and reduce the floating anode slime, thus effectively inhibiting the inclusions of AgCl and Ag colloidal particles. Under the optimized conditions, the Ag content of cathode copper is reduced to less than 7.5 mg/kg.

Key words: cathode copper; Ag inclusion; AgCl; Ag colloidal particles; process optimization

1 Introduction

Most of the anode copper products in the world come from the pyrometallurgy of copper sulfide ores [1,2], which simultaneously reserves a considerable amount of silver (Ag) resource. During the copper smelting process, Ag component tends to be dissolved in copper sulfide and metallic copper, which leads to the enrichment of Ag in anode copper [3,4]. Therefore, the copper matte and the blister copper are regarded as excellent Ag collectors [5−7]. Through an electrorefining process in $CuSO_4$−H_2SO_4 system, most of Ag in the anode copper will enter into the anode slime due to its high chemical stability [8,9]. However, trace amount of Ag may be released to the $CuSO_4$−H_2SO_4 electrolyte in the form of Ag^+ or AgCl and Ag colloidal particles [10], and eventually transports into cathode copper [11−14]. In China, the yield of electrorefining copper reaches up to 9.78×10^6 t with the average Ag content of (10−20) mg/kg [15], which means that at least 97.8 t of Ag will be entrained and taken away by cathode copper annually, thus resulting in evident economic loss. Moreover, the Ag inclusions in cathode copper will also deteriorate the physical and chemical properties of copper products [16]. Therefore, how to effectively reduce the content of Ag in cathode copper is an important issue that needs to be solved urgently.

In industry, a traditional way to control the Ag impurity in cathode copper is to reduce the free Ag^+ by the addition of Cl^- [17]. In this way, the reduction potential of Ag^+ will have a significant negative shift, thus inhibiting the reduction of Ag^+. For example, the studies by NKUNA and POPOOLA [18] showed that the Ag content in cathode copper could be decreased to about 8 mg/kg in the case of 0.02−0.025 g/L Cl^-. However, when Cl^- concentration was higher than 0.025 g/L, the Ag content in cathode copper constantly increased due to the AgCl inclusion [19]. Industrial copper electrolytes usually contain higher concentration of chloride (40−60 mg/L), so the content of Ag in industrial cathode copper usually

Corresponding author: Guo-qu ZHENG, Tel: +86-571-88320429, E-mail: zhenggq@zjut.edu.cn
DOI: 10.1016/S1003-6326(23)66303-4

reaches up to (12−15) mg/kg.

Adjusting electrolytic parameters is another way to reduce Ag impurity in cathode copper. Through theoretical research, BURZYŃSKA [12] revealed that controlling temperature and electrolyte flow rate could partially inhibit the reduction of free Ag^+ at the cathode, but could not limit the inclusion of Ag-containing particles. MA et al [20] found that by regulating electrolysis temperature and current density, the Ag content in cathode copper could be reduced by more than 30% in a copper electrolysis system containing 50 mg/L Cl^-. In addition, some studies showed that the floating anode slime formed by high concentrations of As, Sb, and Bi in the electrolyte could easily entrain AgCl and Ag colloidal particles into cathode copper [21−23].

From previous studies, the presence of Ag in cathode copper is attributed to several facts, including the discharge of free Ag^+ and the mechanical inclusion of AgCl and Ag colloidal particles. However, as of now, the role of polymorphic Ag (Ag^+, AgCl, and Ag colloidal particles) during the cathode process has not been systematically researched. In this work, the reduction behavior of free Ag^+ in copper electrolyte was analyzed by thermodynamic calculation. By associating a series of copper electrolysis experiments, the inclusions of AgCl and Ag colloidal particles on the Ag content of cathode copper were investigated in detail. Sb_2O_3 was utilized to purify the copper electrolyte and remove the floating anode slime which was mainly composed of As, Sb and Bi. The inclusions of AgCl and Ag colloidal particles in cathode copper were successfully inhibited. Combined with electrolysis parameters optimization, the amount of Ag impurity in cathode copper dropped remarkably. This study can provide some theoretical guidance for the optimization of cathode copper electrolysis process and it is of great value and importance in minimizing precious metal resource loss and promoting economic benefits during copper electrorefining.

2 Experimental

2.1 Copper anode and electrolyte

The composition of copper anode used in the electrolysis experiment is shown in Table 1. Among them, the anode copper (2N-Cu) was provided by a nonferrous metal smelter in China, and the high purity copper (6N-Cu) was provided by an electronic technology company in China. Analytical grade $CuSO_4·5H_2O$, H_2SO_4, Sb_2O_3, Bi_2O_3, NaCl, AgCl, arsenic acid (H_3AsO_4, 80%), thiourea and gelatin used in the experiment were purchased from Sinopharm Chemical Reagent Co., Ltd. All the electrolytes were prepared by deionized water.

Electrolytes applied in the experiments are shown in Table 2. Among them, the laboratory electrolyte E-Laboratory (E-Lab) was prepared in the laboratory, and the industrial electrolyte E-Convention (E-Con) was provided by the nonferrous metal smelter in China. E-Con contained high concentrations of As, Sb and Bi. 10 g/L Sb_2O_3 was added to E-Con, stirred at the temperature of 60 °C for 4 h and then filtered to obtain a purified

Table 1 Elemental compositions of anode copper (wt.%)

Anode	Cu	Ag	As	Sb	Bi	Ni	S
2N-Cu	99.37	0.0629	0.1540	0.0278	0.0235	0.0634	0.0051
6N-Cu	99.9999	2.5×10^{-5}	$<1\times10^{-6}$	$<1\times10^{-7}$	$<1\times10^{-7}$	$<1\times10^{-7}$	7×10^{-6}

Table 2 Concentrations of electrolytes (g/L)

Electrolyte	Cu^{2+}	Ag	As	Sb	Bi	Cl^-	H_2SO_4
E-Lab	45.0	$\sim1.2\times10^{-4}$	12	0.51	0.48	0.05	200
E-Con	43.5	2×10^{-4}	12	0.6	0.5	0.05	192
E-Pur	43.3	2×10^{-4}	6	<0.1	<0.1	0.05	189
E-Pur-Sb	43.3	2×10^{-4}	6	0.6	<0.1	0.05	189
E-Pur-Bi	43.3	2×10^{-4}	6	<0.1	0.5	0.05	189
E-Pur-As	43.3	2×10^{-4}	12	<0.1	<0.1	0.05	189

electrolyte E-Purification (E-Pur), in which As, Sb and Bi contents were significantly reduced [24,25]. E-Pur-As, E-Pur-Sb, E-Pur-Sb corresponded to the conditions of elevated As, Sb or Bi content in E-Pur, respectively. All initial Cl^- concentrations in the electrolytes were 50 mg/L (added in the form of NaCl), and were supplemented regularly during the electrolysis process to maintain the Cl^- concentration at a stable level.

2.2 Copper electrolysis experiment

Five comparative experiments were designed to explore the relationship between the three phases of free Ag^+, AgCl and Ag colloidal particles in the electrolyte and the Ag content of cathode copper. In these experiments, the peristaltic pump was used to connect the electrolytic cell and the buffer tank to guarantee the three Ag-containing phases in the electrolyte. E-Lab was used in all experiments. The electrolysis temperature was 62 °C, the current density was 300 A/m^2, and the electrolysis time was 50 h. The obtained cathode copper was firstly soaked in boiling dilute sulfuric acid for 30 min, then rinsed thoroughly with distilled water, dried and stored under nitrogen atmosphere. All electrolysis experiments were repeated three times. The prepared copper cathodes were numbered as Samples A−E respectively, as shown in Fig. 1.

Sample A: 6N-Cu was used as the anode, a filter cloth pocket (pore size <0.1 μm) containing AgCl particles (>20 μm) was placed in the buffer tank, and the cathode was placed in the cloth pocket of the same specification. Only free Ag^+ ($AgCl \rightleftharpoons Ag^+ + Cl^-$) existed in the liquid layer on cathode surface.

Sample B: 6N-Cu was regarded as the anode, and AgCl particles were directly placed in the buffer tank. AgCl and the ionized free Ag^+ ($AgCl \rightleftharpoons Ag^+ + Cl^-$) synchronously existed in the liquid layer on cathode surface.

Sample C: 2N-Cu was used as the anode, and the liquid layer on cathode surface simultaneously contained free Ag^+, AgCl and Ag colloidal particles during electrolysis process.

Sample D: Anode was put into a filter cloth pocket so as to prevent partial AgCl and Ag colloidal particles from entering into the electrolyte. The rest is the same as the preparation of Sample C.

Sample E: Cathode was put into a filter cloth pocket so as to prevent partial AgCl and Ag colloidal particles from entering into the liquid layer of cathode surface. The rest is the same as the preparation of Sample C.

The effects of As, Sb and Bi concentrations on Ag content in cathode copper were studied by comparative experiments in E-Con, E-Pur, E-Pur-Sb, E-Pur-Bi and E-Pur-As. The prepared copper cathodes were numbered as Sample 1−5, respectively. Meanwhile, the influences of Cl^- concentration, electrolysis temperature (50−65 °C), current density (250−350 A/m^2) and electrolyte circulation flow rate (1−6 L/h) were experimentally studied to obtain the optimized electrolysis process factors.

2.3 Characterization

The concentration of various elements in the electrolyte was determined by inductive coupled plasma emission spectrometer (ICP-MS, Perkin Elmer NexION 300X). And Ag content of cathode copper was determined by ICP-MS after cathode copper was nitrated in dilute nitric acid. The elemental composition and distribution of cathode copper were analyzed by using the scanning electron

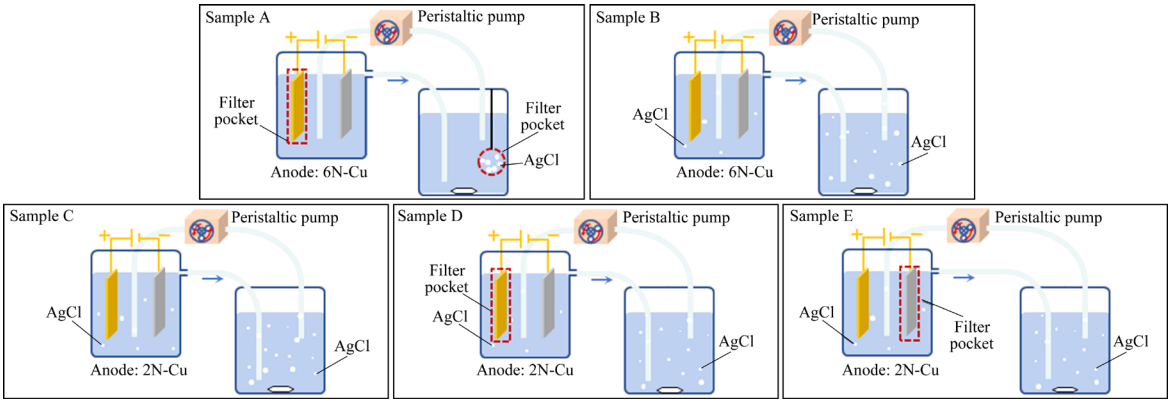

Fig. 1 Schematic diagrams of five comparative experiments

microscope (SEM, Zeiss Sigma 300, operated at 15 kV) equipped with an energy dispersive X-ray spectroscopy (EDS) detector.

3 Results and discussion

3.1 Theoretical research of free Ag^+ reduction

A preliminary analysis by theoretical calculation was conducted to determine the critical concentration of Ag^+ reduction at the potential of Cu^{2+} reduction, and the influence of Cl^- concentration on Ag inclusion was explored simultaneously.

3.1.1 Thermodynamic analysis and species distribution

Since the reduction potential of free Ag^+ in the electrolyte is more positive than that of Cu^{2+}, the addition of Cl-containing additives is a usual and pervasive method to reduce the free Ag^+ in electrolyte and therefore avoid its electrochemical reduction on the cathode. Ag^+ will react with Cl^- to form AgCl precipitate, as exhibited in Reaction (1). When the reaction achieves an equilibrium, the equilibrium concentration of free Ag^+ (C_{Eq}) can be calculated.

$$Ag^+ + Cl^- \rightleftharpoons AgCl\downarrow \quad (1)$$

Because free Ag^+ and Cu^{2+} tend to form various complex compounds with Cl^- [26,27] when the equilibrium concentration of free Ag^+ in the electrolyte is calculated, it is necessary to obtain the corresponding concentration of each complex. It is known that there are independent reactions in the $Cu^{2+}-Ag^+-Cl^--H_2O$ system as shown in Eqs. (2) and (3):

$$Ag^+ + iCl^- = AgCl_i^{1-i} \quad (i=1, 2, 3, 4),$$
$$K_{1,i} = \frac{[AgCl_i^{1-i}]}{[Ag^+][Cl^-]^i} \quad (2)$$

$$Cu^{2+} + jCl^- = CuCl_j^{2-j} \quad (j=1, 2, 3, 4),$$
$$K_{2,j} = \frac{[CuCl_j^{2-j}]}{[Cu^{2+}][Cl^-]^j} \quad (3)$$

All of the activities are replaced by the corresponding concentration in the calculation. According to the principle of simultaneous equilibrium and the law of conservation of mass, the total concentrations of Ag^+, Cu^{2+} and Cl^- can be expressed as follows:

$$[Ag^+]_T = [Ag^+] + \sum_{i=1}^{4} AgCl_i^{1-i} \quad (4)$$

$$[Cu^{2+}]_T = [Cu^{2+}] + \sum_{j=1}^{4} CuCl_j^{2-j} \quad (5)$$

$$[Cl^-]_T = [Cl^-] + \sum_{i=1}^{4} AgCl_i^{1-i} + \sum_{j=1}^{4} CuCl_j^{2-j} \quad (6)$$

where $[Ag^+]_T$, $[Cu^{2+}]_T$, and $[Cl^-]_T$ represent the corresponding total specie concentration, $[Ag^+]$, $[Cu^{2+}]$, and $[Cl^-]$ represent the specific free ion concentration. The $[Ag^+]_T$ and $[Cu^{2+}]_T$ in electrolyte are 0.2 mg/L and 45 g/L, respectively, which are consistent with the industrial electrolyte utilized in the experiments.

Table 3 shows the adoptive complex constants according to the HSC Chemistry 9.0 software database and Lange's Handbook of Chemistry [28]. Substituting the complex constants in Table 3 into Eqs. (4), (5) and (6), the concentration of each species formed by free Cu^{2+} and Ag^+ complexed with Cl^- can be obtained. Figure 2 shows the distributions of each complex at 56 °C. It can be seen from Fig. 2(a) that the addition of $[Cl^-]_T$ can decrease the concentration of free Ag^+, but when $[Cl^-]_T$ increases from 0 to 50 mg/L, the free Ag^+ concentration only decreases from 0.20 to

Table 3 Complex constants (K) of compounds formed between Ag^+, Cu^{2+} and Cl^- at different temperatures

Temperature/°C	Ag				Cu			
	lg $K_{1,1}$	lg $K_{1,2}$	lg $K_{1,3}$	lg $K_{1,4}$	lg $K_{2,1}$	lg $K_{2,2}$	lg $K_{2,3}$	lg $K_{2,4}$
56	3.082	4.910	4.452	2.811	0.476	−0.657	−2.401	−5.061
58	3.071	4.891	4.418	2.760	0.485	−0.642	−2.393	−5.071
60	3.060	4.872	4.385	2.711	0.494	−0.628	−2.383	−5.080
62	3.049	4.854	4.353	2.664	0.503	−0.612	−2.373	−5.087
64	3.039	4.836	4.322	2.617	0.513	−0.597	−2.362	−5.093
66	3.029	4.819	4.291	2.572	0.523	−0.580	−2.350	−5.098

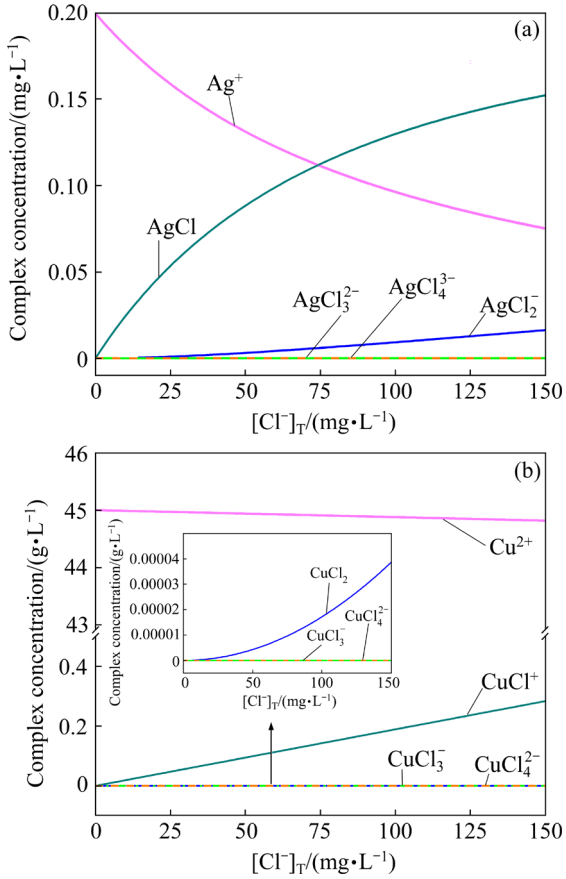

Fig. 2 Distributions of Ag^+ (a) and Cu^{2+} (b) complex compounds with change of $[Cl^-]_T$ ($[Ag^+]_T$=0.2 mg/L, $[Cu^{2+}]_T$=45 g/L, 56 °C)

0.13 mg/L. However, the concentration of $CuCl^+$ increases rapidly, as shown in Fig. 2(b). When the content of $[Cl^-]_T$ is 50 mg/L, the concentration of $CuCl^+$ reaches 95.33 mg/L, indicating that most of the added Cl^- is complexed with Cu^{2+} instead of with Ag^+. At the same time, the concentration of AgCl increases rapidly with the augment of Cl^-.

Equilibrium concentration (C_{Eq}) of free Ag^+ at various $[Cl^-]_T$ and temperatures is calculated, as shown in Fig. 3. It can be seen that with the increase of $[Cl^-]_T$, the concentration of free Ag^+ decreases, and the temperature also has a certain effect on the concentration of free Ag^+. $[Cl^-]_T$ in the industrial electrolyte is usually controlled at about 50 mg/L, so the concentration of free Ag^+ in this case is approximately 0.13 mg/L.

3.1.2 Critical concentration of Ag^+ reduction

According to Nernst equations (Eqs. (7) and (8)), the reduction potentials of Cu^{2+} and Ag^+ at different temperatures can be obtained. The data of standard electrode potential at each temperature comes from the HSC Chemistry 9.0 software database.

$$\varphi_{Cu^{2+}/Cu}=\varphi^0_{Cu^{2+}/Cu}-\frac{RT}{nF}\ln\left(\frac{1}{[Cu^{2+}]}\right) \quad (7)$$

$$\varphi_{Ag^{+}/Ag}=\varphi^0_{Ag^{+}/Ag}-\frac{RT}{nF}\ln\left(\frac{1}{[Ag^{+}]}\right) \quad (8)$$

where R is the molar gas constant (8.314 J/(K·mol); T is the thermodynamic temperature (K); n is the number of electrons transferred in the reaction; F is the Faraday constant (96485 C/mol).

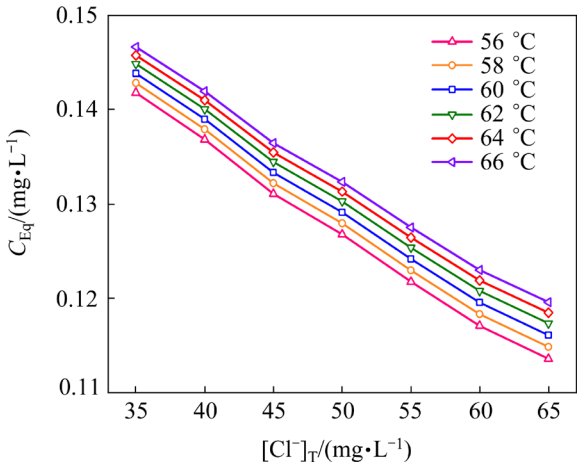

Fig. 3 Equilibrium concentrations (C_{Eq}) of free Ag^+ in copper electrolyte at various $[Cl^-]_T$ and temperatures

When $\varphi_{Ag^{+}/Ag} \geq \varphi_{Cu^{2+}/Cu}$, the cathodic reduction of copper is accompanied with Ag^+ reduction. According to Eqs. (7) and (8), the Ag^+ critical concentration (C_{CRI}) of Ag−Cu co-deposition can be calculated, that is, when the concentration of free Ag^+ exceeds the critical value, Ag^+ reduction will happen. Table 4 shows the reduction potentials of Ag^+ and Cu^{2+} at different temperatures and the corresponding C_{CRI}. As the temperature rises, C_{CRI} increases, indicating that the higher temperature is advantageous for the inhibition of free Ag^+ reduction.

Figure 4 shows the C_{Eq} and C_{CRI} of free Ag^+ at various temperatures. It can be seen that C_{Eq} of free Ag^+ in the electrolyte is much higher than C_{CRI}, that is, the reduction of free Ag^+ on the cathode is thermodynamically feasible under the current conditions. Therefore, under lack of enough Cl-containing additives, the reduction of free Ag^+ is certain to happen. However, excessive amount of Cl^- may deteriorate the quality of cathode copper [29,30], and bring about the corrosion of pipes and equipment at the same time [31].

Table 4 Standard electrode potentials of Ag^+, Cu^{2+} and critical concentration of free Ag^+ (C_{CRI}) at different temperatures

T/℃	$\varphi^0_{Ag^{2+}/Ag}$(vs SHE)/V	$\varphi^0_{Cu^{2+}/Cu}$(vs SHE)/V	C_{CRI}/(mg·L^{-1})
56	0.768	0.337	0.0224
58	0.766	0.337	0.0264
60	0.764	0.337	0.0310
62	0.762	0.337	0.0363
64	0.760	0.337	0.0425
66	0.758	0.337	0.0496

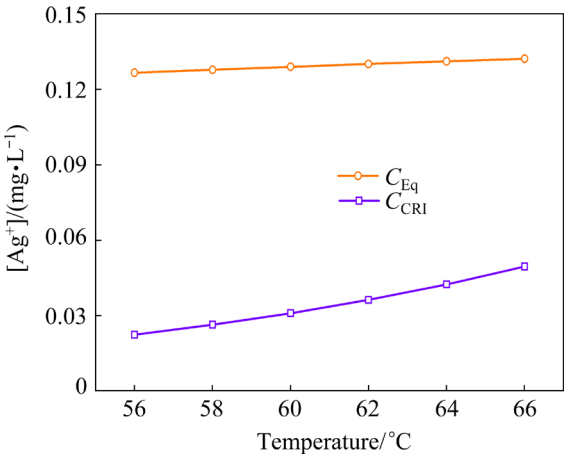

Fig. 4 Equilibrium concentration (C_{Eq}) and critical concentration (C_{CRI}) of free Ag^+ at different temperatures

3.1.3 Ag impurity originated from free Ag^+ reduction

On the premise of only considering the thermodynamic factor and ignoring the influence of kinetic factor and other impurities, the free Ag^+ in the electrolyte which is higher than C_{Eq} will be completely reduced and deposited in cathode copper. Under the conditions of electrolyte volume of 6 m^3, electrolyte circulation flow rate of 30 L/min, current density of 300 A/m^2, electrode area of 70 m^2, and current efficiency of 98%, the theoretical Ag content in cathode copper after electrolysis for 24 h is calculated, as shown in Fig. 5.

Higher temperature and more Cl^- added in electrolyte are beneficial to the control of Ag impurity in cathode copper. The increase of Cl^- can reduce the free Ag^+ [32], while the rising of temperature will lead to the reduction potential of free Ag^+ to shift negatively, both play inhibition role in the Ag^+ reduction. Theoretical calculation results show that the free Ag^+ reduction on the cathode will lead to 5−8 mg/kg Ag impurity in cathode copper.

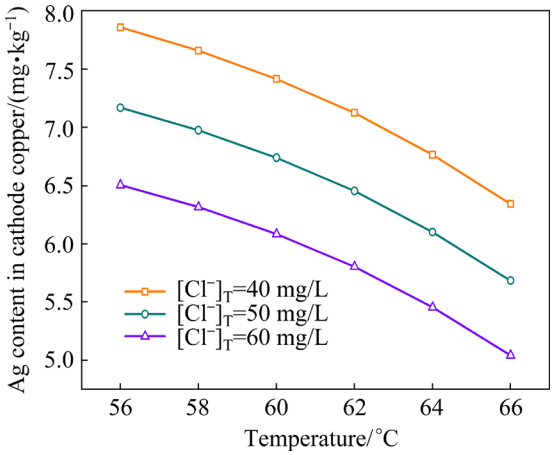

Fig. 5 Theoretical Ag content in cathode copper after electrolysis for 24 h

3.2 Characteristics of Ag inclusions during copper electrolysis

During copper electrolysis, there may exist several forms of Ag ingredients in electrolyte, including free Ag^+, AgCl and Ag colloidal particles. Five groups of comparative experiments were designed to investigate the behavior of different Ag-containing species and their effects on the Ag content in cathode copper. Figure 6 presents the variation of Ag content in cathode copper under different electrolysis conditions. It should be announced that Sample A possesses the limited Ag content of 7.4 mg/kg, and only free Ag^+ exists on the cathode surface at this time, that is, the Ag in Sample A originates from the electrochemical reduction of free Ag^+. This result is basically consistent with that obtained by theoretical calculations. The Ag content in Sample B is 13.8 mg/kg, which is 6.4 mg/kg higher than that in Sample A. At this time, the cathode surface contains both free Ag^+ and AgCl, indicating that the inclusion of AgCl is also the main factor leading to the high Ag content in cathode copper. The Ag content in cathode copper of Sample C is as high as 17 mg/kg, which is due to the combined impact of the discharge of free Ag^+ and the inclusion of AgCl and Ag colloidal particles. The difference between Samples C and D is that the anode is sleeved with a filter cloth pocket, for the aim to prevent the Ag colloidal particles generated by anodic dissolution from entering the electrolyte. However, according to the experimental results, the drop of Ag content (16 mg/kg) in cathode copper is not obvious, that is, the filter cloth pocket cannot completely obstruct

the infiltration of Ag colloidal particles. The preparation of Sample E is different from that of Sample C in that the cathode is sleeved with filter cloth pocket to prevent AgCl and Ag colloidal particles in electrolyte from entering the liquid layer on cathode surface. On this occasion, the content of Ag in cathode copper obviously decreases (11 mg/kg), indicating that the AgCl inclusions can be hindered by the filter cloth pocket.

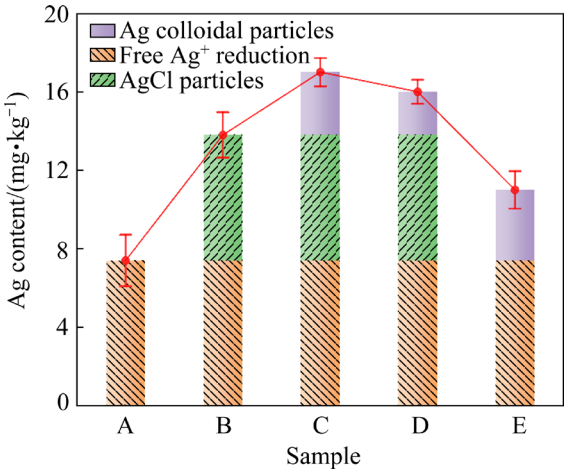

Fig. 6 Sources of Ag in cathode copper under different electrolysis conditions

It can be seen from the above experiments that the reduction of free Ag^+, the inclusions of AgCl and Ag colloidal particles are indeed the facts affecting the Ag content in cathode copper, and among them, the reduction of free Ag^+ and the inclusion of AgCl play the major role. Prior research has shown that the inclusion of AgCl and Ag colloidal particles are greatly affected by the floating anode slime of As, Sb and Bi [8,21]. Generally, AgCl and Ag colloidal particles in the electrolyte will precipitate at the bottom of cell slowly after they are formed. But when there is enough floating anode slime, AgCl and Ag colloidal particles will be adsorbed by the anode slime, and finally reach the cathode surface with the flowing electrolyte. A schematic diagram illustrating the behaviors of three Ag-containing phases during copper electrolysis is shown in Fig. 7.

Besides the previously mentioned method of reducing free Ag^+, taking effective measures to remove the floating anode slime may be also conductive to the control of Ag impurities in cathode copper.

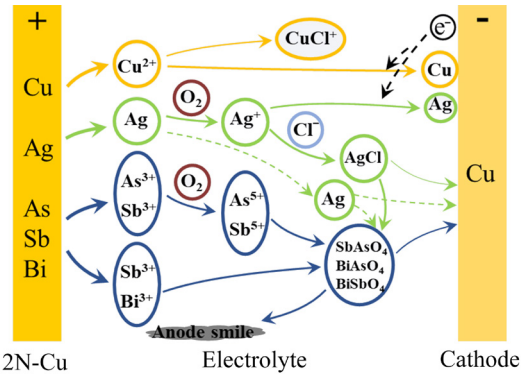

Fig. 7 Schematic diagram showing behavior of three Ag-containing phases during copper electrolysis

3.3 Control of Ag impurity in cathode copper

3.3.1 Effects of As, Sb and Bi impurities in electrolyte

Figure 8 shows the Ag content of cathode copper in assigned electrolyte with different compositions. Sample 1 was prepared in the industrial electrolyte E-Con with higher As, Sb and Bi concentrations, and Sample 2 was prepared in the purified electrolyte E-Pur with low As, Sb and Bi concentrations. The concentrations of Sb, Bi and As in E-Pur were increased to 0.6, 0.5 and 12.0 g/L, respectively, to obtain Samples 3, 4 and 5. It can be seen from Fig. 8 that Sample 1 obtained in E-Con possesses the highest Ag content, reaching 17 mg/kg. According to the results shown in Fig. 3, the Ag content can be divided as: 7.4 mg/kg from the reduction of free Ag^+, 6.4 mg/kg from the inclusion of AgCl and 3.2 mg/kg from the inclusion of Ag colloidal particles, that is, the electrochemical reduction of free Ag^+, the inclusions of AgCl and

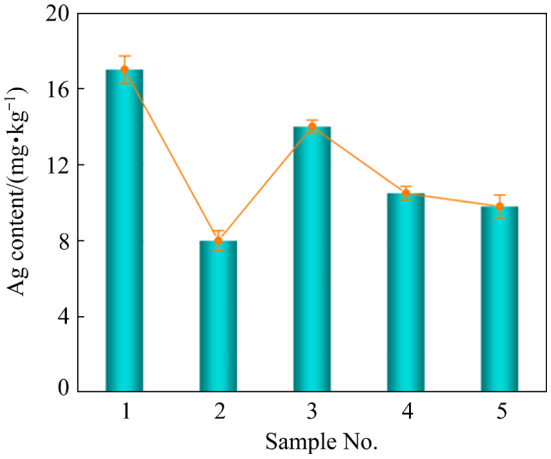

Fig. 8 Ag content of cathode copper in assigned electrolyte with different compositions (Anode: 2N-Cu; 300 A/m^2; 62 °C)

Ag colloidal particles are all the sources of Ag impurity in cathode copper. The Ag content in Sample 2 is 8 mg/kg. Electrolysis conditions of Samples 1 and 2 are consistent except for the chemical composition of electrolyte. It should be announced that Ag content from the reduction of free Ag^+ in Sample 2 is equal to that in Sample 1. So, the drop of Ag content in Sample 2 is attributed to the less inclusions of AgCl and Ag colloidal particles. This result indicates that decreasing the As, Sb and Bi concentrations in electrolyte is effective for the control of Ag content in cathode copper, since the amount of floating anode slime such as antimonate and arsenate drops evidently [22], and accordingly the amount of AgCl and Ag colloidal particles entrained by floating anode slime will also decline. The Ag contents of Samples 3, 4 and 5 are 14, 10.5 and 9.8 mg/kg, respectively, which are higher than that in Sample 2. Sb is considered to have the greatest influence on the formation of floating anode slime [22,33]. The higher the concentration of Sb, the larger the amount of floating anode slime is generated. Thus, the Ag content of Sample 3 obtained by using E-Pur-Sb with higher Sb concentration is higher than that of Samples 4 and 5 obtained by using the electrolyte with lower Sb concentration. This also reflects the entrainment characteristics of AgCl and Ag colloidal particles in floating anode slime.

Figure 9 shows the SEM images of cathode copper obtained in three different electrolytes. From Figs. 9(a) and (e), the surface morphologies of Samples 1 and 3 are relatively similar, and the grain size of copper substrate does not change significantly. However, Sample 2 presents a much compact surface due to the finer grains in Fig. 9(c), which indicates that the decrease of Sb concentration could optimize the grain size of cathode copper and the smoother surface must be unfavorable for the mechanical entrainment of impurities. Combined with the EDS results in Table 5, it is found that the contents of Ag, As, Sb and Bi in Sample 2 are the lowest. Meanwhile, it can be seen from Figs. 9(b, d, f) that the regions where have high As, Sb and Bi contents also accumulate large amount of Ag and Cl, i.e. the AgCl and Ag inclusions in the cathode copper are closely related to As, Sb and Bi. Based on this, it can be concluded that the floating anode slime composed of As, Sb, and Bi is a carrier to entrain the Ag-containing impurities into cathode copper. Therefore, the electrolyte purification process to remove As, Sb and Bi impurities in electrolyte will be an efficient way to inhibit the inclusions of AgCl and Ag colloidal particles in cathode copper.

3.3.2 Effect of electrolysis temperature

Figure 10 shows the Ag content of cathode copper and the current efficiency at assigned temperatures. With the temperature rising, the cathode copper obtained in two electrolytes (E-Pur and E-Con) presents different upward trends in Ag content. The Ag content of cathode copper prepared in E-Pur increases slightly with the increase of temperature. When the temperature is 56 ℃ (Fig. 10(a)), the Ag content of cathode copper is as low as 5.8 mg/kg by using E-Pur, and it only increases to 9.5 mg/kg at 66 ℃. According to the results of thermodynamic calculation, the reduction amount of free Ag^+ will decrease with temperature rising, so the increase of Ag content with the increase of temperature must originate from the other factors, such as the inclusions of AgCl and Ag colloidal particles. The solution viscosity varies with the increase of electrolysis temperature [34], as a result, the diffusion of AgCl and Ag colloidal particles with floating anode slime becomes easier at higher temperatures, which leads to more inclusions of AgCl and Ag colloidal particles in cathode copper [35]. Besides, arsenate and antimonate are prone to be formed at higher temperatures, leading to larger amount of floating anode slime in the electrolyte and promoting the entrainment of AgCl and Ag colloidal particles in cathode copper. Due to the lower Sb content in E-Pur than that in E-Con, floating anode slime in E-Pur is less, so that the increment of Ag content is smaller.

In Fig. 10(b), the current efficiency of E-Pur is slightly lower than that of E-Con at low temperatures. But when the electrolysis temperature is above 62 ℃, the current efficiency of E-Pur and E-Con is pretty close, reaching up to about 95.8% [36].

3.3.3 Effect of current density

Figure 11 shows the Ag content of cathode copper and the corresponding current efficiency at assigned current density. It can be seen from Fig. 11(a) that when the current density is 200 A/m^2, cathode copper with the Ag content of 7 mg/kg can be obtained by using E-Pur. With the increase of

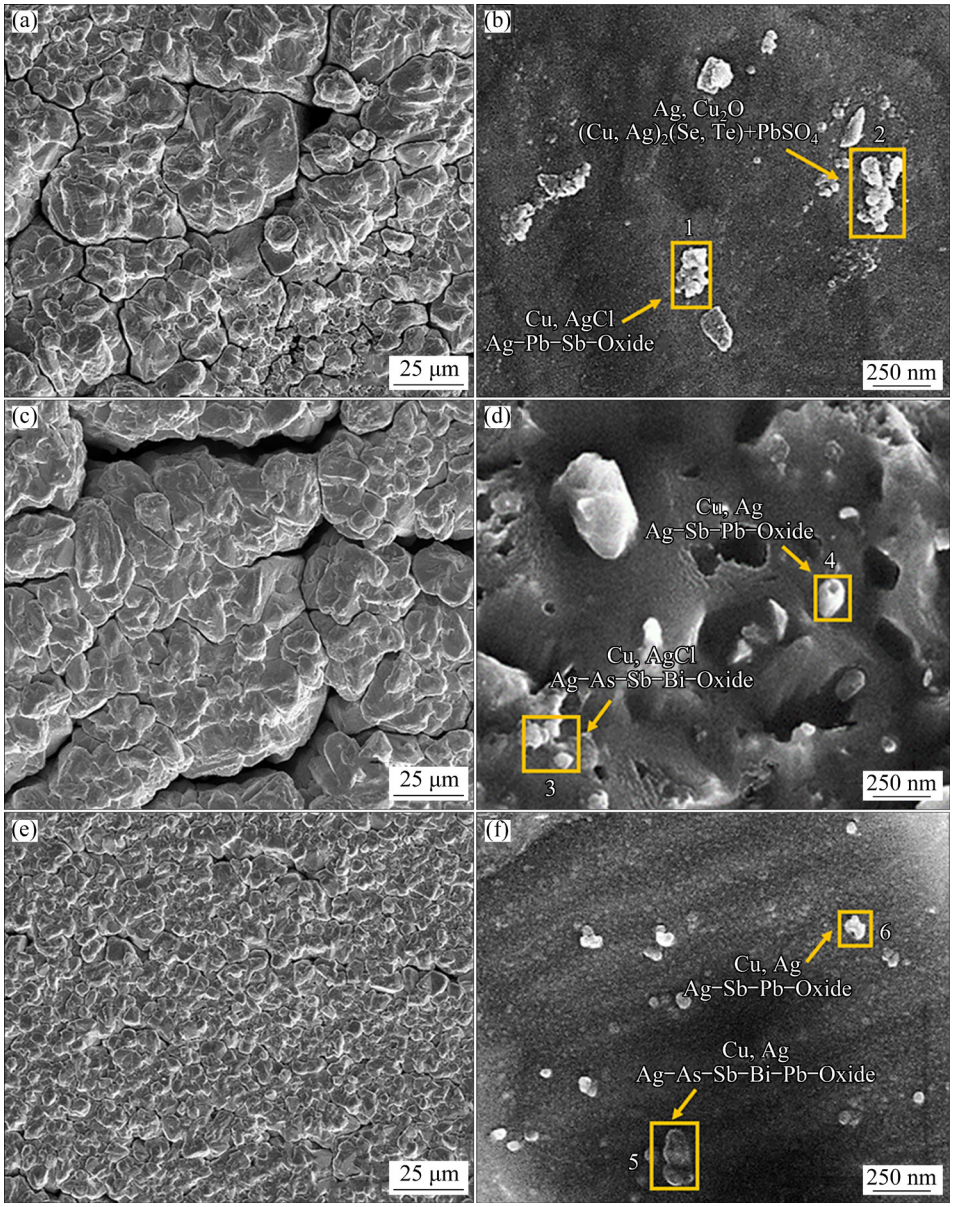

Fig. 9 SEM images of cathode copper obtained in three different electrolytes: (a, b) Sample 1, E-Con; (c, d) Sample 2, E-Pur; (e, f) Sample 3, E-Pur-Sb

Table 5 EDS analysis results of cathode copper (wt.%)

Spot in Fig. 9	Cu	Ag	As	Sb	Bi	Cl	Se	Te	Pb	O
1	99.24	0.21	0.08	0.09	–	0.14	–	–	0.03	0.14
2	99.38	0.12	0.01	0.05	–	–	0.02	0.01	0.06	0.20
3	99.72	0.04	0.03	0.02	0.02	0.01	–	–	0.02	0.10
4	99.78	0.07	–	0.04	–	–	–	–	0.01	0.03
5	99.49	0.11	0.02	0.07	0.02	0.04	–	–	0.04	0.12
6	99.56	0.07	–	0.05	–	–	–	–	0.05	0.09

current density, the Ag content of cathode copper obtained with the two electrolytes increases. The Ag content of cathode copper obtained with E-Pur increases from 7 to 13 mg/kg, while that obtained with E-Con varies considerably from 14 to 22 mg/kg. At high current density, the active reduction site on cathode surface increases rapidly, while Cu^{2+} migration to cathode surface is

controlled by the diffusion limitation [37,38]. The increase of Cu^{2+}-depleted area makes the electroreduction of free Ag^+ easier. In E-Con electrolyte, high Ag content of cathode copper is due to the excessive generation of floating anode slime, which entraps Ag-containing charged particles and migrates to the cathode surface rapidly at high current density. In Fig. 11(b), the current efficiency of E-Pur and E-Con declines gradually with increasing current density, from more than 96% at 200 A/m^2 to about 94% at 400 A/m^2. When the current density increases, the voltage drop consumed by the electrolyte resistance and that of the cathode and anode polarization increase accordingly [39]. The higher current density could also induce the concentration polarization of Cu^{2+} at electrode/electrolyte interface and aggravate the hydrogen-evolving side reaction [40,41].

3.3.4 Effect of electrolyte circulation flow rate

Figure 12 shows the effect of circulation flow rate on Ag content and current efficiency. With the circulation flow rate increasing, mass transfer of free Ag^+ is accelerated, which thereby benefits its electroreduction on cathode. But for AgCl and Ag colloidal particles, they may be more easily stripped from the cathode surface at fast circulation flow rate. Due to the joint action of the above two factors, the Ag content shows a trend of first decreasing and then increasing (Fig. 12(a)). Besides, Ag content of cathode copper prepared in E-Pur is lower than that prepared in E-Con at the same circulation flow rate, which is attributed to the role of floating anode slime. The migration of AgCl and Ag colloidal particles is more difficult in E-Pur. Figure 12(b) shows the effect of circulation flow rate on current efficiency, which obviously illustrates the same trend caused by the circulation flow rate in E-Pur and E-Con. The increase of the circulation flow rate can effectively mitigate the concentration polarization of Cu^{2+} [42], leading to the increase of current efficiency [43,44].

In summary, the Ag content of cathode copper can be effectively reduced by using E-Pur with low As, Sb and Bi concentrations. When the

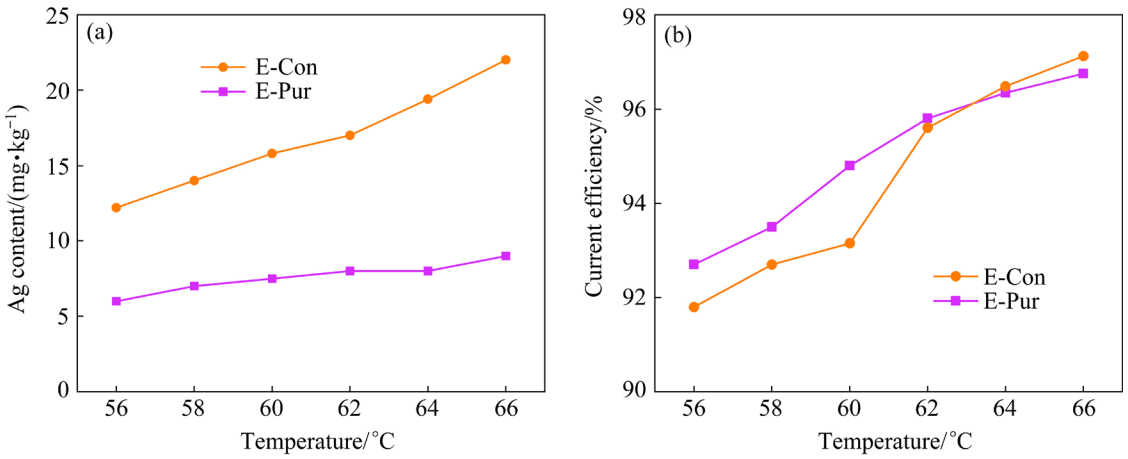

Fig. 10 Effect of temperature on Ag content (a) and current efficiency (b) of cathode copper

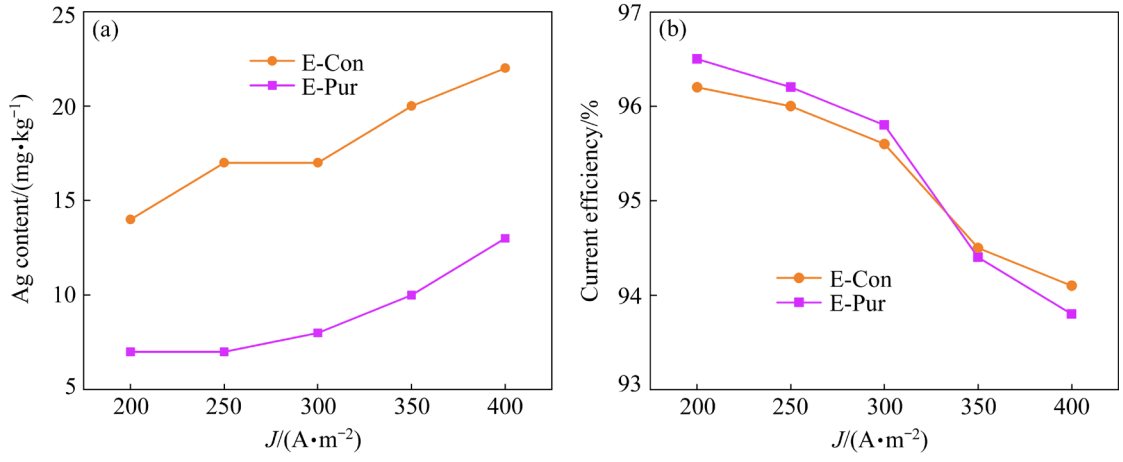

Fig. 11 Effect of current density on Ag content (a) and current efficiency (b) of cathode copper

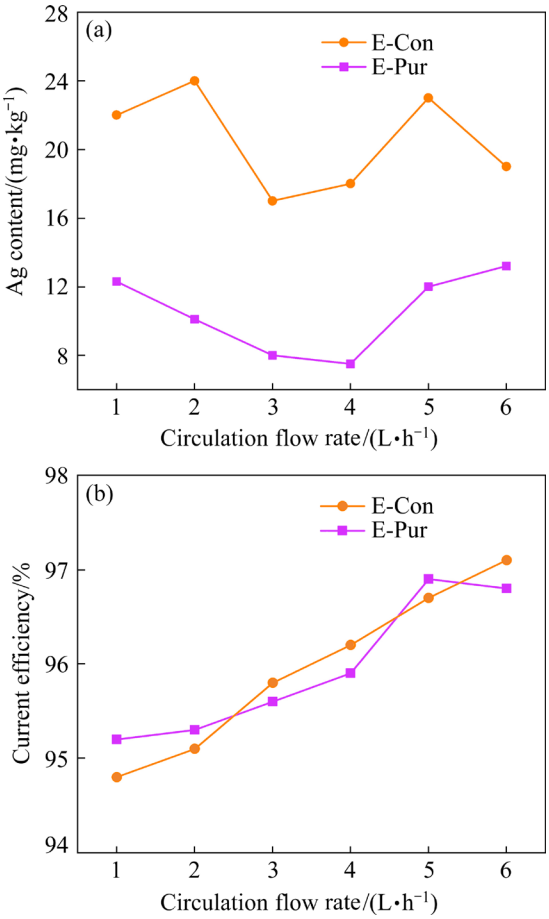

Fig. 12 Effect of circulation flow rate on Ag content (a) and current efficiency (b) of cathode copper

concentration of Cl^- is 50 mg/L, the electrolysis temperature is 62 °C, the current density is 300 A/m^2, and the circulation flow rate of electrolyte is 4 L/h, the cathode copper with Ag content of 7.5 mg/kg can be obtained. The Ag content can be reduced by more than 50% compared with E-Con. This part of Ag will eventually enter into the floating anode slime and further recycling will be conducted through hydrometallurgy and other processes [45−47]. By this way, the loss of noble metal Ag caused by the entrainment of cathode copper can be minimized and the quality of cathode copper will also be improved.

4 Conclusions

(1) The effects of Ag^+, AgCl and Ag colloidal particles on the Ag content of cathode copper during electrolysis process were clarified through experimental studies and theoretical calculation. The regulation mechanism of Ag content in cathode copper was revealed, and a novel process for efficiently reducing Ag content of cathode copper was proposed.

(2) The Ag impurity in cathode copper originates from the electroreduction of free Ag^+ and the inclusions of AgCl and Ag colloidal particles according to a series of experiments to simulate the copper electrorefining system.

(3) By the adoption of Sb_2O_3 to purify copper electrolyte, As, Sb and Bi impurities in electrolyte as well as the floating anode slime can be greatly reduced. By this way, the inclusion of AgCl and Ag colloidal particles in cathode copper was efficiently inhibited.

(4) The Ag content of cathode copper obtained by E-Con is about 17 mg/kg when the Cl^- concentration is 50 mg/L, while E-Pur with low As, Sb and Bi concentrations can effectively reduce the inclusions of AgCl and Ag colloidal particles in cathode. By optimized electrolysis conditions, i.e. electrolysis temperature of 62 °C, current density of 300 A/m^2, Cl^- concentration of 50 mg/L and electrolyte circulation flow rate of 4 L/h, the cathode copper with Ag content of 7.5 mg/kg can be obtained with current efficiency higher than 95%.

Acknowledgments

This work was supported by the National Natural Science Foundation of China (No. 51374185).

References

[1] ANGGARA S, BEVAN F, HARRIS R C, HARTLEY J M, FRISCH G, JENKIN G R T, ABBOTT A P. Direct extraction of copper from copper sulfide minerals using deep eutectic solvents [J]. Green Chemistry, 2019, 21(23): 6502−6512.

[2] GUO Xue-yi, CHEN Yuan-lin, WANG Qin-meng, WANG Song-song, TIAN Qing-hua. Copper and arsenic substance flow analysis of pyrometallurgical process for copper production [J]. Transactions of Nonferrous Metals Society of China, 2022, 32(1): 364−376.

[3] LIU Gong-qi, WU Yu-feng, TANG Ai-jun, PAN De-an, LI Bin. Recovery of scattered and precious metals from copper anode slime by hydrometallurgy: A review [J]. Hydrometallurgy, 2020, 197: 105460.

[4] WENZL C, FILZWIESER I, MORI G, PESL J. Investigations on anode quality in copper electrorefining [J]. BHM Berg- und Hüttenmännische Monatshefte, 2008, 153(3): 91−96.

[5] LIU Jian-hua, GUI Wei-hua, XIE Yong-fang, YANG Chun-hua. Dynamic modeling of copper flash smelting

process at a smelter in China [J]. Applied Mathematical Modelling, 2014, 38(7/8): 2206−2213.

[6] MOATS M S, WANG S J, KIM D. A review of the behavior and deportment of lead, bismuth, antimony and arsenic in copper electrorefining [C]//Proceedings of Symposium on Hydrometallurgy, Electrometallurgy and Materials Characterization. Hoboken, NJ, USA: John Wiley & Sons, 2012: 1−21.

[7] LI Jia-yuan, WANG Tao, SUN Zhong-hui, WU Jian-jian, SHEN Dian-ling, YUAN Qing, LI Xiao-xuan, CHEN Jun. Treatment of high arsenic content lead copper matte by a pressure oxidative leaching combined with cyclone and vertical electro-deposition method [J]. Separation and Purification Technology, 2018, 199: 282−288.

[8] ZENG Wei-zhi, WERNER J, FREE M L. Experimental studies on impurity particle behavior in electrolyte and the associated distribution on the cathode in the process of copper electrorefining [J]. Hydrometallurgy, 2015, 156: 232−238.

[9] ZENG Wei-zhi, WANG Shi-jie, FREE M L. Experimental studies of the effects of anode composition and process parameters on anode slime adhesion and cathode copper purity by performing copper electrorefining in a pilot-scale cell [J]. Metallurgical and Materials Transactions B, 2016, 47(5): 3178−3191.

[10] CHEN T T, DUTRIZAC J E. A mineralogical study of the deportment and reaction of silver during copper electrorefining [J]. Metallurgical and Materials Transactions B, 1989, 20(3): 345−361.

[11] KUCHARSKA-GIZIEWICZ E A, MACKINNON D J. Electrochemical behaviour of silver-containing copper anodes under simulated electrorefining conditions [J]. Journal of Applied Electrochemistry, 1996, 26(1): 51−57.

[12] BURZYŃSKA L. Influence of electrolysis parameters on the silver content of cathodic copper [J]. Hydrometallurgy, 2000, 55(1): 17−33.

[13] DONG Zhong-lin, JIANG Tao, XU Bin, YANG Jun-kui, CHEN Yan-zhu, LI Qian, YANG Yong-bin. Comprehensive recoveries of selenium, copper, gold, silver and lead from a copper anode slime with a clean and economical hydrometallurgical process [J]. Chemical Engineering Journal, 2020, 393: 124762.

[14] OSTANIN N I, RUDOY V M, DEMIN I P, OSTANINA T N, NIKITIN V S. Statistical analysis of the distribution of impurities during copper electrorefining [J]. Russian Journal of Non-Ferrous Metals, 2021, 62(5): 501−507.

[15] KASUNO T, KITADA A, SHIMOKAWA K, MURASE K. Suppression of silver dissolution by contacting different metals during copper electrorefining [J]. Journal of MMIJ, 2014, 130: 65−69. (in Japanese)

[16] LU Su-jun, LI Juan, CHEN Da-lin, SUN Wei, ZHANG Juan, YANG Yue. A novel process for silver enrichment from Kaldo smelting slag of copper anode slime by reduction smelting and vacuum metallurgy [J]. Journal of Cleaner Production, 2020, 261: 95−104.

[17] BOUNOUGHAZ M, MANZINI M, GHALI E. Behaviour of copper anodes containing oxygen, silver and selenium impurities during electro-refining [J]. Canadian Metallurgical Quarterly, 1995, 34(1): 21−26.

[18] NKUNA E H, POPOOLA A P I. Effect of chloride electrolyte additive on the quality of electrorefined copper cathode [J]. Procedia Manufacturing, 2019, 35: 789−794.

[19] WANG Xue-wen, CHEN Qi-yuan, YIN Zhou-lan, WANG Ming-yu, XIAO Bing-rui, ZHANG Fan. Homogeneous precipitation of As, Sb and Bi impurities in copper electrolyte during electrorefining [J]. Hydrometallurgy, 2011, 105(3/4): 355−358.

[20] MA Jun, LI Jian, LUO Jin-song, YE Wen-chun. Practice of reducing contents of silver in cathode copper in Yunnan Copper Industry Co., Ltd [J]. China Nonferrous Metallurgy, 2014, 45(3): 24−29. (in Chinese)

[21] ZENG Wei-zhi, WANG Shi-jie, FREE M L. Experimental and simulation studies of electrolyte flow and slime particle transport in a pilot scale copper electrorefining cell [J]. Journal of the Electrochemical Society, 2016, 163(5): E111−E122.

[22] JAFARI S, KIVILUOMA M, KALLIOMÄKI T, KLINDTWORTH E, AJI A T, AROMAA J, WILSON B P, LUNDSTRÖM M. Effect of typical impurities for the formation of floating slimes in copper electrorefining [J]. International Journal of Mineral Processing, 2017, 168: 109−115.

[23] GONZÁLEZ TORRES A I, MOATS M S, RÍOS G, RODRÍGUEZ ALMANSA A, SÁNCHEZ-RODAS D. Removal of Sb impurities in copper electrolyte and evaluation of As and Fe species in an electrorefining plant [J]. Metals, 2021, 11(6): 902.

[24] WANG Xing-ming, WANG Xue-wen, LIU Biao, WANG Ming-yu, WANG Hua-guang, LIU Xue-hui, ZHOU Shen-fan. Promotion of copper electrolyte self-purification with antimonic oxides [J]. Hydrometallurgy, 2018, 175: 28−34.

[25] XIAO Fa-xin, CAO Dao, MAO Jian-wei, SHEN Xiao-ni, REN Feng-zhang. Role of trivalent antimony in the removal of As, Sb, and Bi impurities from copper electrolytes [J]. International Journal of Minerals, Metallurgy, and Materials, 2013, 20(1): 9−16.

[26] WELHAM N J, KELSALL G H, DIAZ M A. Thermodynamics of Ag−Cl−H_2O, Ag−Br−H_2O and Ag−I−H_2O systems at 298 K [J]. Journal of Electroanalytical Chemistry, 1993, 361(1/2): 39−47.

[27] ZAMFIRESCU C, NATERER G F, ROSEN M A. Chemical exergy of electrochemical cell anolytes of cupric/cuprous chlorides [J]. International Journal of Hydrogen Energy, 2017, 42(16): 10911−10924.

[28] DEAN J A. Lange's handbook of chemistry [J]. Materials and Manufacturing Processes, 1990, 5(4): 687−688.

[29] SUN M, O'KEEFE T J. The effect of additives on the nucleation and growth of copper onto stainless steel cathodes [J]. Metallurgical Transactions B, 1992, 23(5): 591−599.

[30] SHAO W, PATTANAIK G, ZANGARI G. Influence of chloride anions on the mechanism of copper electrodeposition from acidic sulfate electrolytes [J]. Journal of the Electrochemical Society, 2007, 154(4): D201−D207.

[31] LI Heng, WANG Xiao-wei, YIN Xu-zhong, YANG Xin-yu, TANG Jian-qun, GONG Jian-ming. Corrosion and electrochemical investigations for stainless steels in molten Solar Salt: The influence of chloride impurity [J]. Journal of Energy Storage, 2021, 39: 102675.

[32] KALLIOMÄKI T, AROMAA J, LUNDSTRÖM M. Modeling the effect of composition and temperature on the conductivity of synthetic copper electrorefining electrolyte [J]. Minerals, 2016, 6(3): 59.
[33] PETKOVA E N. Mechanisms of floating slime formation and its removal with the help of sulphur dioxide during the electrorefining of anode copper [J]. Hydrometallurgy, 1997, 46(3): 277−286.
[34] LI Jian, FAN Xue-ping, WANG Da-jian. One of the physicochemical property of copper electrolyty: The viscosity of copper electrolyte [J]. Non-ferrous Mining and Metallurgy, 2003, 19(4): 23−27. (in Chinese)
[35] KALLIOMAKI T, AJI A T, RINTALA L, AROMAA J, LUNDSTROM M. Models for viscosity and density of copper electrorefining electrolytes [J]. Physicochemical Problems of Mineral Processing, 2017, 53: 1023−1037.
[36] PANDA B, DAS S C. Electrowinning of copper from sulfate electrolyte in presence of sulfurous acid [J]. Hydrometallurgy, 2001, 59(1): 55−67.
[37] MOATS M S, HISKEY J B, COLLINS D W. The effect of copper, acid, and temperature on the diffusion coefficient of cupric ions in simulated electrorefining electrolytes [J]. Hydrometallurgy, 2000, 56(3): 255−268.
[38] KALLIOMÄKI T, WILSON B P, AROMAA J, LUNDSTRÖM M. Diffusion coefficient of cupric ion in a copper electrorefining electrolyte containing nickel and arsenic [J]. Minerals Engineering, 2019, 134: 381−389.
[39] SUN Ya-feng, REN Bing-zhi, WANG Hong-dan, XIA Wen-tang, DENG You-ming, XIANG Wei, WANG Lei. Effect of process conditions on power consumption of copper electrorefining [J]. Non-ferrous Metals (Smelting Part), 2018(6): 5−8. (in Chinese)
[40] WANG Yan, LI Bo, WEI Yong-gang, WANG Hua. Effect of Zn^{2+} on the extraction of copper by cyclone electrowinning from simulated copper-containing electrolyte [J]. Separation and Purification Technology, 2022, 282: 120014.
[41] WANG Ming-yong, WANG Zhi, GUO Zhan-cheng. Preparation of electrolytic copper powders with high current efficiency enhanced by super gravity field and its mechanism [J]. Transactions of Nonferrous Metals Society of China, 2010, 20(6): 1154−1160.
[42] NIKITIN V S, OSTANINA T N, RUDOI V M, KULOSHVILI T S, DARINTSEVA A B. Features of hydrogen evolution during electrodeposition of loose deposits of copper, nickel and zinc [J]. Journal of Electroanalytical Chemistry, 2020, 870: 114230.
[43] WANG Hong-dan, WANG Qian, XIA Wen-tang, REN Bing-zhi. Effect of jet flow between electrodes on power consumption and the apparent density of electrolytic copper powders [J]. Powder Technology, 2019, 343: 607−612.
[44] HEMMATI H, MOHEBBI A, SOLTANI A, DANESHPAJOUH S. CFD modeling of the electrolyte flow in the copper electrorefining cell of Sarcheshmeh copper complex [J]. Hydrometallurgy, 2013, 139: 54−63.
[45] KHALEGHI A, GHADER S, AFZALI D. Ag recovery from copper anode slime by acid leaching at atmospheric pressure to synthesize silver nanoparticles [J]. International Journal of Mining Science and Technology, 2014, 24(2): 251−257.
[46] KHANLARIAN M, RASHCHI F, SABA M. A modified sulfation−roasting−leaching process for recovering Se, Cu, and Ag from copper anode slimes at a lower temperature [J]. Journal of Environmental Management, 2019, 235: 303−309.
[47] HYK W, KITKA K. Highly efficient and selective leaching of silver from electronic scrap in the base-activated persulfate−ammonia system [J]. Waste Management, 2017, 60: 601−608.

铜电解精炼过程中银夹杂物的迁移规律及控制

冯闻宇，曹华珍，沈宇坤，徐圣航，张惠斌，郑国渠

浙江工业大学 材料科学与工程学院，杭州 310014

摘　要：通过热力学计算分析游离 Ag^+的还原行为，并通过电解实验研究 Ag 夹杂的控制工艺。结果表明，游离 Ag^+的放电还原无法避免。As、Sb 和 Bi 所形成的漂浮阳极泥的夹带作用是造成 AgCl 和 Ag 胶粒在阴极铜中形成夹杂的关键因素。采用 Sb_2O_3 净化铜电解液，减少漂浮阳极泥，从而有效抑制了 AgCl 和 Ag 胶粒在阴极铜中的夹杂。在优化条件下，阴极铜中银含量降至 7.5 mg/kg 以下。

关键词：阴极铜；银夹杂；AgCl；Ag 胶粒；工艺优化

(Edited by Wei-ping CHEN)